Biexcitons in two-dimensional systems with spatially separated electrons and holes

A. D. Meyertholen and M. M. Fogler
Department of Physics, University of California–San Diego, 9500 Gilman Drive, La Jolla, California 92093, USA
(Received 21 August 2008; revised manuscript received 27 October 2008; published 10 December 2008)

The binding energy and wave functions of two-dimensional indirect biexcitons are studied analytically and numerically. It is proven that stable biexcitons exist only when the distance between electron and hole layers is smaller than a certain critical threshold. Numerical results for the biexciton binding energies are obtained using the stochastic variational method and compared with the analytical asymptotics. The threshold interlayer separation and its uncertainty are estimated. The results are compared with those obtained by other techniques, in particular, the diffusion Monte Carlo method and the Born-Oppenheimer approximation.

DOI: 10.1103/PhysRevB.78.235307 PACS number(s): 78.67.De, 71.35.Cc, 71.15.Nc

I. PROBLEM AND MAIN RESULTS

The physics of cold excitons—bound states of electrons and holes in semiconductors—has attracted much attention recently. Cooling the excitons has become possible by confining electrons and holes in separate two-dimensional (2D) quantum wells, which greatly increases their lifetime. A number of intriguing phenomena has been demonstrated for such "indirect" excitons, including long-range transport,[1–6] macroscopic spatial ordering,[3] and spontaneous coherence.[7] Theoretical work on these phenomena is ongoing; see Ref. 8 for review. Further progress in this field requires an improved understanding of exciton interactions.

Despite being charge neutral, indirect excitons possess a dipole moment ed, where d is the separation of the electron and hole quantum wells. As a result, interaction of two excitons at large distances r is dominated by their dipolar repulsion,

$$V(r) = \frac{e^2}{\kappa}\frac{d^2}{r^3}, \tag{1}$$

where κ is the dielectric constant of the semiconductor. At short distances exchange and correlation effects are also important. The interaction may even become attractive over a range of r. In this case two excitons can form a bound state—a biexciton. The corresponding binding energy is defined by

$$E_B = 2E_X - E_{XX}, \tag{2}$$

where E_X and E_{XX} are the ground-state energies of the exciton and biexciton, respectively.

While observations of biexcitons in single quantum well structures ($d=0$) have been described multiple times,[9–16] no such reports exist for the $d>0$ case. A recent theoretical work[17] has attributed the lack of experimental signatures of indirect biexcitons to extreme smallness of their binding energies. In this paper we verify and improve all previously known estimates of E_B. In particular, we show that $E_B(d)$ is positive, i.e., the biexciton is stable, only for d smaller than some critical value d_c; see Fig. 1. Typical experimental parameters[8,18] fall on the $d>d_c$ part of the diagram.

In our calculations we adopt the simplifying assumption that the effective masses m_e and $m_h \geq m_e$ of electrons and holes are constant and isotropic. We also treat the quantum wells as 2D layers of zero thickness. We find it convenient to measure distances in units of the effective electron Bohr radius and energies in units of the effective Rydberg,

$$a_e = \frac{\hbar^2\kappa}{m_e e^2}, \quad \mathrm{Ry}_e = \frac{1}{2}\frac{e^2}{\kappa a_e}, \tag{3}$$

respectively. With these conventions, the four-particle system of two electrons and two holes is described by the Hamiltonian $H_{XX}=T+U$, where

$$T = T_1 + T_2, \quad T_j = -\nabla_j^2 - \sigma\nabla_{\mathbf{R}_j}^2, \tag{4}$$

$$U = \frac{2}{|\mathbf{r}_1 - \mathbf{r}_2|} + \frac{2}{|\mathbf{R}_1 - \mathbf{R}_2|} - \sum_{ij} v(\mathbf{r}_i - \mathbf{R}_j, d), \tag{5}$$

$$v(\mathbf{r}, d) = \frac{2}{\sqrt{|\mathbf{r}|^2 + d^2}}. \tag{6}$$

Here $\mathbf{r}_i$ and $\mathbf{R}_i$ are 2D coordinates of the electrons and the holes, respectively, $\nabla_j = d/d\mathbf{r}_j$, and

$$\sigma = m_e/m_h \tag{7}$$

is the mass ratio. Similarly, the single-exciton Hamiltonian is

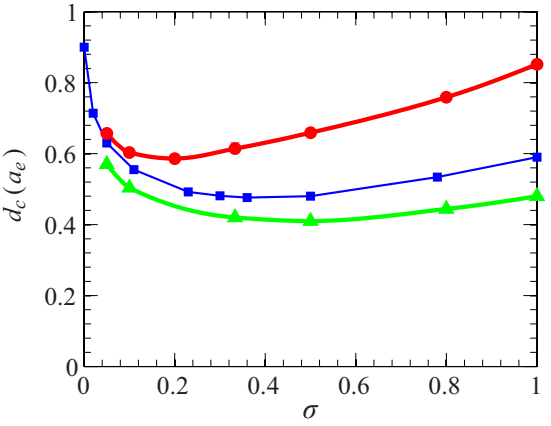

FIG. 1. (Color online) Critical interlayer separation d_c above which the biexciton is unstable as a function of the electron-hole mass ratio σ. The circles are our results. The squares are from Ref. 24. The triangles correspond to d above which $E_B(d)$ drops below $10^{-3}\mathrm{Ry}_e$, making biexcitons irrelevant in experimental practice.

$$H_X = T_1 + v(\mathbf{r}_1 - \mathbf{R}_1, d). \tag{8}$$

The problem is characterized by two dimensionless parameters: d and σ. The electron-hole symmetry entails

$$E_a\left(\frac{1}{\sigma}, d\right) = \sigma E_a\left(\sigma, \frac{d}{\sigma}\right), \quad a = X \text{ or } XX, \tag{9}$$

and so it is sufficient to consider $0 \leq \sigma \leq 1$.

The case of $d=0$ (direct excitons) has been studied extensively.[19–21] In contrast, high-accuracy calculations of E_B for $d>0$ have been carried out only in the aforementioned Ref. 17. The authors of that work employed the diffusion quantum Monte Carlo (DMC) method. Away from $d=0$, they were able to fit their results for $\sigma=1$ and $\sigma=1/2$ to the exponential

$$E_B(d) \approx \alpha e^{-\beta d}. \tag{10}$$

This result is surprising. Equation (10) seems to imply that the biexcitons are stable at any d, i.e., $d_c=\infty$. On the other hand, physical intuition and previous approximate calculations[22,23] suggest that d_c should be finite. A more recent work[24] has reached the same conclusion. In this paper we present rigorous analytical arguments and essentially exact numerical results proving that $d_c \leq 1$ at all σ; see Fig. 1.

Since d_c is finite, interpolation formula (10) must overestimate the binding energy at large d. We show that near the biexciton dissociation threshold,

$$d_c - d \ll D, \tag{11}$$

where $D \sim 1$ for $\sigma \sim 1$ and $D \sim \exp(-\sigma^{-1/2})$ for $\sigma \ll 1$, function $E_B(d)$ behaves as

$$E_B \simeq E_0 e^{-D/(d_c-d)}. \tag{12}$$

This equation resembles the well-known expression for the energy ε of a bound state in a weak 2D potential $V(r)$. Such a state exists if

$$W \equiv \frac{M}{2\pi\hbar^2}\int d^2 r V(r) < 0, \tag{13}$$

where M is the mass of the particle. Near the threshold $W \to 0$ one finds[25]

$$|\varepsilon| \propto e^{-1/|W|}, \quad |W| \ll 1. \tag{14}$$

The exciton-exciton interaction potential $V(r)$ in general does not satisfy the condition of the perturbation theory $V(r)r^2 \ll \hbar^2/M$, with $M=m_e+m_h$. Therefore, Eq. (14) does not literally apply here. Nevertheless, the physical origins of the exponential dependence in Eqs. (12) and (14) are the same; see Sec. II B.

We verify and complement the above analytical results numerically using the stochastic variational method (SVM).[26] The SVM has proven to be a powerful technique for computing the energies of few-particle systems.[27] For example, it has given the best estimates of E_B for direct biexcitons,[19,20] $d=0$. Our calculations are largely in excellent agreement with those of Ref. 17; see Fig. 2 and Table I. Thus, Eq. (10) is certainly useful as an interpolation formula for not too large d. However, near the estimated d_c, our results favor Eq. (12) over Eq. (10). Since the SVM is variational, we can be sure that it is more reliable when it gives a larger E_B than other methods.

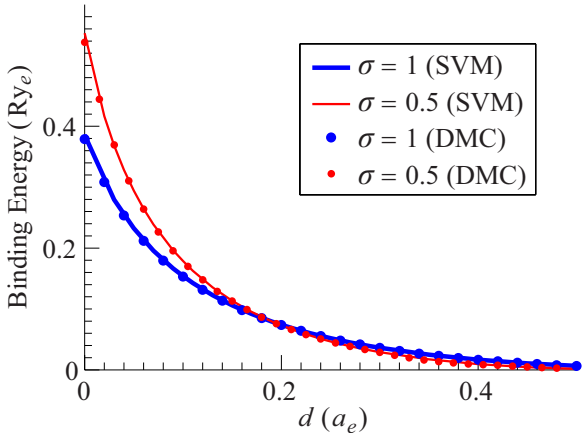

FIG. 2. (Color online) Binding energy vs the distance between the quantum wells for the mass ratios $\sigma=1$ and 0.5. Our results based on the SVM are shown as the solid lines. The dots are results of the DMC calculation from Ref. 17.

The remainder of the paper is organized as follows. In Sec. II we derive a few analytical bounds on E_B and asymptotic formula (12). Numerical calculations are presented in Sec. III. Section IV is devoted to discussion and comparison with results in previous literature. Some details of the derivation are given in Appendixes A and B.

II. ANALYTICAL RESULTS

In this section we approach the biexciton problem by analytical methods. Since the exact solution seems out of reach, the best one can do is to consider certain limits where suitable control parameters exist. Below we examine three of them. First, we study large-d excitons. We prove that they cannot bind into a stable biexciton. Second, we consider the immediate vicinity $d_c-d \ll 1$ of the dissociation threshold d_c. We derive the asymptotical formula for the binding energy, Eq. (12), which is valid for arbitrary σ. Finally, we analyze the case $\sigma \ll 1$.

A. Exciton interaction at large d

The absence of stable biexcitons at large d is due to the lack of binding in the classical limit, which is realized at such d. Indeed, if we temporarily change the length units to d and energy units to $e^2/\kappa d$, then the potential energy U in Eq. (5) becomes d independent while the kinetic energy T acquires the extra factor $a_e/d \ll 1$ compared to Eq. (4). Hence, the potential energy dominates. A rigorous proof that $d_c < \infty$ can be constructed by dealing with the quantum and many-body aspects of the problem separately. The many-body part is handled at the classical level. Thereafter the quantum corrections are included. With further analysis, both parts of the argument can be reduced to simpler problems for which controlled approximations exist.

Since the Earnshaw theorem does not apply in two dimensions, the absence of a stable classical biexciton is not im-

TABLE I. Biexciton binding energies in units of Ry_e from the previous ("DMC," Ref. 17) and present ("SVM") works.

$\sigma=1$			$\sigma=0.5$		
$d(a_e)$	DMC	SVM	$d(a_e)$	DMC	SVM
0.000	0.3789	0.3858	0.000	0.5381	0.5526
0.020	0.3084	0.3089	0.015	0.4443	0.4450
0.040	0.2538	0.2546	0.030	0.3695	0.3689
0.060	0.2118	0.2133	0.045	0.3104	0.3109
0.080	0.1794	0.1807	0.060	0.2639	0.2649
0.100	0.1532	0.1542	0.075	0.2265	0.2275
0.120	0.1315	0.1324	0.090	0.1956	0.1966
0.140	0.1135	0.1141	0.105	0.1696	0.1707
0.160	0.0982	0.0986	0.120	0.1477	0.1487
0.180	0.0851	0.0855	0.135	0.1291	0.1299
0.200	0.0738	0.0742	0.150	0.1130	0.1136
0.220	0.0640	0.0644	0.165	0.0989	0.0995
0.240	0.0556	0.0559	0.180	0.0865	0.0872
0.260	0.0483	0.0485	0.195	0.0757	0.0764
0.280	0.0418	0.0420	0.210	0.0663	0.0670
0.300	0.0361	0.0363	0.225	0.0580	0.0586
0.320	0.0311	0.0313	0.240	0.0507	0.0512
0.340	0.0267	0.0270	0.255	0.0443	0.0447
0.360	0.0229	0.0231	0.270	0.0385	0.0389
0.380	0.0195	0.0197	0.285	0.0333	0.0337
0.400	0.0165	0.0167	0.300	0.0286	0.0291
0.420	0.0140	0.0141	0.315	0.0241	0.0250
0.440	0.0117	0.0118	0.330	0.0200	0.0214
0.460	0.0096	0.0097	0.345	0.0165	0.0182
0.480	0.0078	0.0079	0.360	0.0135	0.0154
0.500	0.0063	0.0065	0.375	0.0112	0.0129
0.520	0.0051	0.0052	0.390	0.0096	0.0107
0.540	0.0040	0.0040	0.405	0.0087	0.0087
0.560	0.0030	0.0031	0.420	0.0076	0.0071
0.580	0.0021	0.0023	0.435	0.0064	0.0056
0.600	0.0013	0.0017	0.450	0.0051	0.0044
0.620	0.0007	0.0012	0.465	0.0039	0.0033
0.640	0.0002	0.0007	0.480	0.0027	0.0024

mediately obvious. However, we verified it following these steps. The classical ground state is the global minimum of the potential energy. We can do the minimization over the electron positions $\mathbf{r}_1$ and $\mathbf{r}_2$ first. Letting $\mathbf{R}$ be the distance between the holes,

$$\mathbf{R} = \mathbf{R}_1 - \mathbf{R}_2, \tag{15}$$

then the energy function to minimize is (in the original unit convention)

$$U_R = \frac{2}{|\mathbf{r}_1 - \mathbf{r}_2|} + \frac{2}{R} - \sum_{\substack{j=1,2 \\ \mathbf{t}=\pm\mathbf{R}/2}} v(\mathbf{r}_j - \mathbf{t}, d). \tag{16}$$

It can be shown that for all R the lowest energy is achieved when the in-plane coordinates of the four charges fall on a straight line; see Fig. 3. Forming a cross is the only other viable alternative, but it always has a higher energy. For the linear geometry of the system, numerically exact results for $U_{\min}(R,d) \equiv \min_{\mathbf{r}_1,\mathbf{r}_2} U_R$ are obtained trivially. The plot of $V_{\mathrm{cl}}(R) \equiv U_{\min}(R,d) + (4/d)$ is shown in Fig. 3. This combination can be thought of as the classical limit of the exciton interaction potential $V(R)$. Function V_{cl} monotonously de-

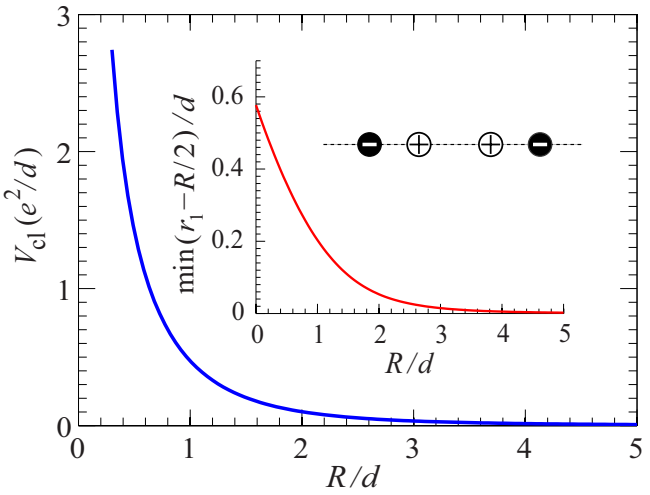

FIG. 3. (Color online) Main panel: Ground-state energy $U_{\min}$ vs the separation R of holes for a pair of classical excitons. In this state all four charges are on the same straight line. Inset: In-plane distance between nearest electrons and holes vs R.

creases with R and achieves its global minimum at $R=\infty$. This means that classical excitons do not form a bound state.

At large R, function $V_{cl}(R)$ follows dipolar interaction law (1) with the quadrupolar, etc., corrections:

$$V_{cl}(R,d) = \frac{2d^2}{R^3} - \frac{3}{2}\frac{d^4}{R^5} + \mathcal{O}\left(\frac{d^6}{R^7}\right), \quad R \gg d. \tag{17}$$

Quantum corrections due to the zero-point motion about the classical ground state are not able to compete with the dipolar repulsion when d is large; see Appendix A. Therefore, there is a critical $d_c=d_c(\sigma)$ above which a stable biexciton does not exist.

B. Binding energy near d_c

In this subsection we examine the biexciton state near the dissociation threshold d_c for arbitrary σ. It is easy to understand that in this regime the biexciton orbital wave function Ψ should have a long tail extending to large distances away from the center of mass of the system. Inside of this tail the configurations of electrons and holes resemble a pair of well-separated individual excitons. Therefore, at $r \gg 1$, where r is the distance between the centers of mass of two such excitons, Ψ takes the asymptotic form

$$\Psi = [1 + (-1)^s P_{12}]\Phi(\mathbf{r}) \prod_{j=1,2} \phi_\sigma(\mathbf{r}_j - \mathbf{R}_j), \tag{18}$$

$$\mathbf{r} = \frac{1}{1+\sigma}\mathbf{R} + \frac{\sigma}{1+\sigma}(\mathbf{r}_1 - \mathbf{r}_2). \tag{19}$$

Here s is the total electron spin, ϕ_σ is the ground-state wave function of a single exciton with mass ratio σ, and operator P_{12} exchanges $\mathbf{r}_1$ and $\mathbf{r}_2$. Let us assume, for simplicity, that holes are spin-1/2 particles. Then the wave function Φ of the relative motion must have the parity $\Phi(-\mathbf{r})=(-1)^{s+S}\Phi(\mathbf{r})$, where S is the total spin of the holes. Our goal in this subsection is to determine the behavior of Φ at large r and use it to derive Eq. (12).

We proceed, as usual, by expanding Φ into partial waves of angular momenta m (m and $s+S$ must be simultaneously odd or even). The equation for the radial wave function $\chi_m(r)$ reads

$$-\frac{1}{r}\frac{d}{dr}r\frac{d\chi_m}{dr} + \left[\varkappa^2 + \mu V(r) + \frac{m^2}{r^2}\right]\chi_m = 0, \tag{20}$$

where $\varkappa$ and μ are defined by

$$\varkappa = \sqrt{\mu E_B}, \quad \mu = \frac{1+\sigma}{2\sigma}. \tag{21}$$

At small distances, potential $V(r)$ is either ill defined or complicated, but for $r \gg d$ it obeys the dipolar law $V(r)=2d^2/r^3$ [Eq. (1)]. From this, it is easy to see that $\mu V(r) r^2 \ll 1$ at $r \gg b$ with b given by

$$b = 8\mu d^2. \tag{22}$$

At such r the potential energy V acts as a small perturbation.[25] Therefore, $\chi_m(r)$ coincides with the wave function of a free particle,

$$\chi_m(r) = c_1 K_m(\varkappa r), \quad r \gg b. \tag{23}$$

Note that b is either on the order of or much larger than d because $\mu \geq 2$ and $d \simeq d_c \sim 1$.

Sufficiently close to the critical d, we have $\varkappa \ll 1/b$. In this case there exists an interval of distances $b \ll r \ll b^{1/3}\varkappa^{-2/3}$ where we can drop the term $\varkappa^2$ in Eq. (20) compared to $\mu V(r)$. After this, Eq. (20) admits the solution

$$\chi_m(r) = I_{2m}\left(\sqrt{\frac{b}{r}}\right) - 4c_2 K_{2m}\left(\sqrt{\frac{b}{r}}\right), \tag{24}$$

where $I_{2m}(z)$ and $K_{2m}(z)$ are the modified Bessel functions of the first and the second kinds, respectively.[28] The unit coefficient for $I_{2m}(z)$ and the factor of (-4) in front of c_2 are chosen for the sake of convenience. The ground-state solution is obtained for $m=0$. Using the asymptotic expansion[28] of I_0 and K_0 in Eqs. (23) and (24) and demanding them to be consistent with one another, we find for $m=0$ and $b \ll r \ll \varkappa^{-1}$ the following:

$$\chi_0 = 1 - 2c_2\left[\ln\left(\frac{4r}{b}\right) - 2\gamma\right] + \mathcal{O}\left(\frac{b}{r}\right), \tag{25}$$

$$c_2 = -\frac{1}{6\gamma + 2\ln(b\varkappa/8)} = \frac{1}{\ln(E_0/E_B)}, \tag{26}$$

where

$$E_0 = \frac{8}{e^{6\gamma}}\left(\frac{\sigma}{1+\sigma}\right)^3 \frac{1}{d^4}. \tag{27}$$

Here $\gamma=0.577\ldots$ is the Euler-Mascheroni constant.[28] Equation (25) specifies the boundary condition to which the solution for χ_0 in the near field, $r \lesssim b$, must be matched.

At $d=d_c$, both $\varkappa$ and c_2 vanish. Wave function $\chi_0(r)$ at small $\varkappa$ can be viewed as the wave function for $d=d_c$ per-

turbed by the small change in the boundary condition in the far field, $r \gtrsim b$, and by another perturbation,

$$\varkappa^2 + \mu V(r)|_{d_c}^{d},$$

in the near field, $r \lesssim b$. To the first order in these perturbations we have

$$E_B = -Ac_2 + B(d, \varkappa^2), \tag{28}$$

where A is a constant and B is a smooth function subject to the condition $B(d_c, 0) = 0$. Expanding B to the first order in $d_c - d$ and $\varkappa^2$, we arrive at the transcendental equation for E_B:

$$\left(1 - \mu \frac{\partial B}{\partial \varkappa^2}\right) E_B + \frac{A}{\ln(E_0/E_B)} = -\frac{\partial B}{\partial d}(d_c - d). \tag{29}$$

The solution cannot be written in terms of elementary functions. However, at $E_B \ll E_0$ the logarithmic term gives the sharpest dependence on E_B. In this limit, the first term on the left-hand side of Eq. (29) can be dropped. Now this equation can be easily solved to recover Eq. (12) with

$$D = \frac{A}{C}, \quad C = -\frac{\partial B}{\partial d}. \tag{30}$$

The coefficients A and C must be determined from the solution of the inner problem. For $\sigma \ll 1$ part of this task can be accomplished analytically, as explained later in this section. For $\sigma \sim 1$ a numerical solution, such as the one discussed in Sec. III, seems to be the only alternative.

Our results comply with a general theorem,[29] which states that in the asymptotic limit $k = i\varkappa \to 0$ the scattering phase shift $\delta(k)$ satisfies the equation

$$(\pi/2)\cot\,\delta(k) = \ln(k/2) + f(k^2), \tag{31}$$

where $f(z)$ is some analytic function. This theorem is valid for a general short-range potential in two dimensions. For a bound state $\cot\,\delta(k)$ should be replaced by i, leading to

$$\ln(\mu E_B/4) + 2f(-\mu E_B) = 0, \tag{32}$$

which is in agreement with our Eq. (29). Our derivation has the advantage of showing that the proper dimensionless combination in the argument of the logarithm is E_B/E_0 and that asymptotic behavior (12) is realized at $E_B \ll E_0$.

C. Binding energy for small mass ratios

Although the electron-hole mass ratio is not truly small in typical semiconductors, it is interesting to examine the case $\sigma \ll 1$ from the theoretical point of view. At such σ the exciton interaction potential V can be meaningfully defined at all distances using the Born-Oppenheimer approximation (BOA).[30,31] In addition, the radial wave function can be computed everywhere with accuracy of $\mathcal{O}(\sigma)$.

The distance r between excitons is no longer a physically reasonable variable when the four particles approach each other closely and their partitioning into excitons becomes ambiguous. In the BOA this problem is mitigated by selecting R—the distance between the heavy charges—to be the radial coordinate of choice. The ground-state biexciton wave function is taken to be

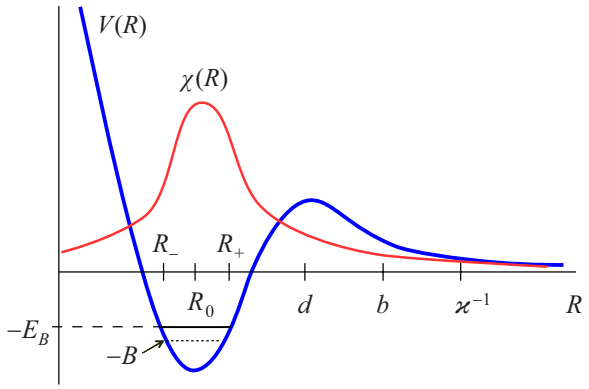

FIG. 4. (Color online) Sketch of the interaction potential $V(R)$ and the exciton wave function $\chi(R)$ for the Born-Oppenheimer limit $\sigma \ll 1$.

$$\Psi = \chi(R)\varphi(\mathbf{R}, \mathbf{r}_1, \mathbf{r}_2), \tag{33}$$

where φ is the ground state of two interacting electrons subject to the potential of two holes fixed at positions $\mathbf{R}_{1,2} = \pm \mathbf{R}/2$:

$$H_{\mathrm{BOA}}\varphi = [-\nabla_1^2 - \nabla_2^2 + U_R(\mathbf{r}_1, \mathbf{r}_2)]\varphi = U_{\mathrm{BOA}}\varphi. \tag{34}$$

Here $U_{\mathrm{BOA}}(R)$ is the corresponding energy. In turn, $\chi(R)$ is found from

$$-\frac{1+\sigma}{R}\frac{d}{dR}R\frac{d\chi}{dR} + \mu[U_{\mathrm{BOA}}(R) - E_{\mathrm{BOA}}]\chi = 0. \tag{35}$$

The BOA is known to have $\mathcal{O}(\sigma)$ accuracy. In principle, it can be systematically improved.[32] However, since below we will be solving Eq. (35) by means of the quasiclassical approximation, which itself is known to be accurate only up to $\mathcal{O}(\sigma)$, this is unwarranted.

Dropping all inessential $\mathcal{O}(\sigma)$ terms, we can simplify Eq. (35) as follows:

$$-\frac{1}{R}\frac{d}{dR}R\frac{d\chi}{dR} + [\varkappa^2 + \mu V(R)]\chi = 0, \tag{36}$$

$$V(R) \equiv U_{\mathrm{BOA}}(R) - U_{\mathrm{BOA}}(\infty). \tag{37}$$

Our task is to solve this equation with boundary conditions $|\chi(0)| < \infty$ at the origin and

$$\chi(R) \simeq I_0\left(\sqrt{\frac{b}{R}}\right) - 4c_2 K_0\left(\sqrt{\frac{b}{R}}\right) \tag{38}$$

at $b \ll R \ll b^{1/3}\varkappa^{-2/3}$, with c_2 given by Eq. (26).

We reason as follows: in order to have a bound state, potential $V(R)$ must be negative over some range of R. It can be shown that this occurs in a single contiguous interval; see Fig. 4 and Sec. III. Inside of this interval there is a classically allowed region, $\mu V(R) < -\varkappa^2$, where function $\chi(R)$ reaches a maximum. As we approach the dissociation threshold, this region shrinks. Near the threshold it becomes very narrow, so that the quadratic approximation

$$\mu V(R) \simeq -\varkappa^2 + \frac{1}{2}\mu V''(R-R_-)(R-R_+) \tag{39}$$

becomes legitimate. Here R_- and R_+ are the turning points. To construct the desired solution we simply need to match $\chi(R)$ in the classical region, $R_- < R < R_+$, inside the tunneling region, $R_+ \ll R \ll b$, and in the far field, $R \gg b$. Details of this calculation are outlined in Appendix B. The result is

$$A = 4\left(\frac{\pi}{e}\sigma V''\right)^{1/2} \exp(-2S_0), \tag{40}$$

$$S_0 = \frac{1}{\sqrt{2\sigma}}\int_{R_+}^{\infty} dR\sqrt{V(R)}, \tag{41}$$

$$B = |V(R_0)| - \sqrt{\sigma V''}, \tag{42}$$

where $R_0=(R_++R_-)/2$ is the point where $V(R)$ has the minimum.

Equations (30) and (40) imply that the coefficient D in Eq. (12) and so range (11) of d where Eq. (12) applies are proportional to the exponentially small factor e^{-2S_0} at $\sigma \ll 1$. We expect that D grows with σ and by extrapolation reaches a number on the order of unity at $\sigma \sim 1$.

A few other properties of function $d_c(\sigma)$ can also be deduced analytically. For example, Eq. (42) implies that

$$d_c(0) - d_c(\sigma) \propto \sqrt{\sigma}, \quad \sigma \ll 1. \tag{43}$$

Hence, $d_c(\sigma)$ has an infinite derivative at $\sigma=0$ and so initially decreases with σ. At some σ, however, $d_c(\sigma)$ must start to increase. Indeed, due to the electron-hole symmetry [Eq. (9)], the combination $d_c(\sigma)/(1+\sigma)$ must have a vanishing derivative at $\sigma=1$. Therefore,

$$d_c'(1) = d_c(1)/2 > 0. \tag{44}$$

Finally, we have a strict upper bound (similar to that in Ref. 33)

$$d_c(\sigma) \le (1+\sigma)d_c(0). \tag{45}$$

All of these properties are borne out by our Fig. 1. Still, a purely analytical solution of the biexciton problem does not appear to be possible at any σ. In Sec. III, we approach it by numerical calculations.

III. NUMERICAL SIMULATIONS

In order to verify our analytical predictions and other results in the literature,[17,24] we have carried out a series of numerical calculations using the SVM. The SVM is a highly accurate variational method with all parts of the Coulomb interaction (Hartree, exchange, and correlation) accounted for. To implement this method we customized the published SVM computer code[34] for the problem at hand. In the SVM one adopts a nonorthogonal basis of correlated Gaussians in the form[27]

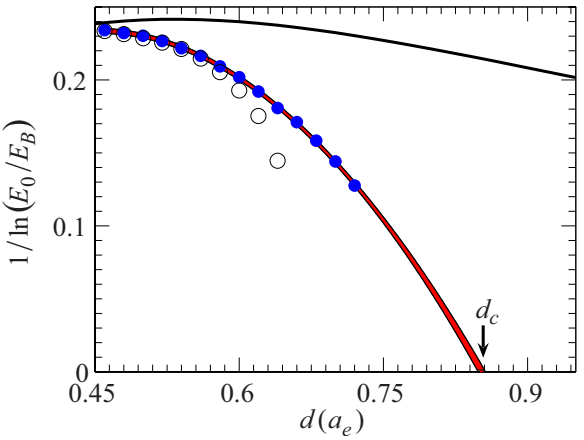

FIG. 5. (Color online) Logarithmic plot of the biexciton binding energy as a function of d for $\sigma=1$. Our results are shown as the filled symbols; the open circles are from Ref. 17. The thicker line is the fit to Eq. (48), which yields $d_c=0.87\pm0.01$ with a 95% confidence level. The other line is Eq. (10) with α and β from Ref. 17.

$$G_n = \exp\left(-\frac{1}{2}\mathbf{x}^\dagger \mathbf{B}_n \mathbf{x}\right), \tag{46}$$

from which a variational wave function of given electron and hole spins (S and s, respectively) is constructed:

$$\Psi = \mathcal{A}[G_n(\{\mathbf{r}_\nu\})\Upsilon_{S,s}]. \tag{47}$$

Here $\mathbf{x}$ is a 3×1 vector of Jacobi coordinates (linear combinations of differences in particle coordinates in which the kinetic energy separates), $\mathbf{B}_n$ is a positive-definite 3×3 matrix, $\mathcal{A}$ is the antisymmetrizer, and $\Upsilon_{S,s}$ is the spin wave function. All our SVM calculations are done for the spin-singlet state $S=s=0$. Note that G_n corresponds to the zero total momentum of the system.

The number of basis states is grown incrementally until the energy is converged or the prescribed basis dimension (typically 700) is reached. At each step a new quadratic form $\mathbf{B}_n$ is generated randomly. If adding the corresponding function G_n to the basis improves the variational energy significantly, this G_n is kept. Otherwise, a new $\mathbf{B}_n$ is generated by varying some of its matrix elements. Details can be found in Refs. 27 and 34.

Our numerical results for $\sigma=0.5$ and $\sigma=1$ are given in Table I and plotted in Fig. 2. In Fig. 5 we replot the binding energy E_B for $\sigma=1$ in a form suitable for testing Eq. (12):

$$\frac{1}{\ln(E_0/E_B)} = \frac{d_c-d}{D} + \frac{(d_c-d)^2}{D_1}. \tag{48}$$

Here we take into account one more term in the Taylor expansion of the right-hand side of Eq. (28) compared to Eq. (29). Extrapolation of the data to $E_B=0$ gives us d_c. The uncertainties in this parameter are estimated by imposing a 95% confidence level on the fit coefficients d_c, D, and D_1. The same procedure has been applied to several other mass ratios in the interval $0.1<\sigma\le1$. The results for d_c are shown in Fig. 1. Their comparison with other results in the literature will be addressed in Sec. IV.

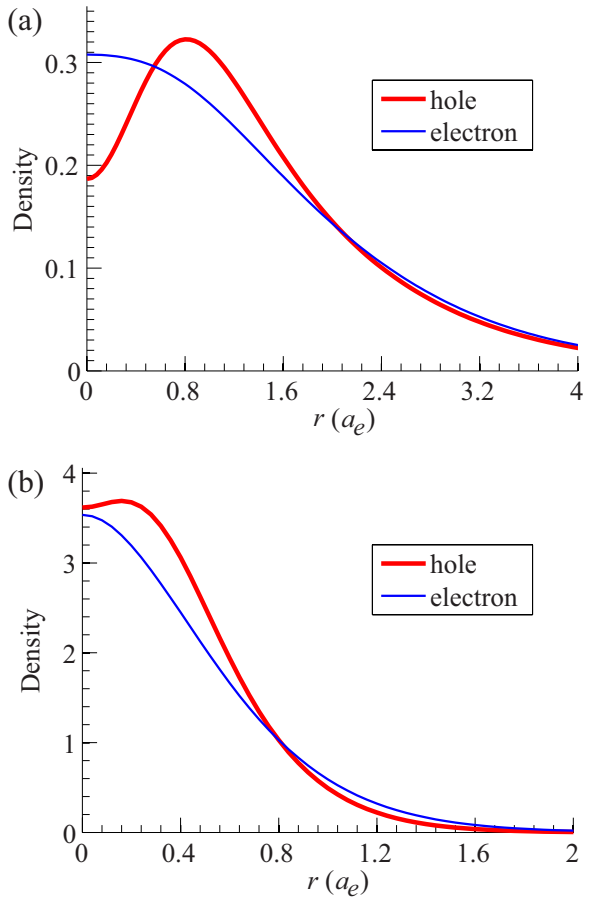

FIG. 6. (Color online) (a) Electron and hole density vs the distance to the center of mass in a biexciton with $\sigma=0.5$ and $d=0.3$. (b) Same as (a) for $\sigma=0.5$ and $d=0.0$.

At $\sigma \leq 0.1$ range (11) of d where Eq. (12) applies is exponentially small. Even with our highly accurate numerical method, we were not able to probe this range. Thus, we assumed that the nonanalytical correction $Ac_2(E_B)$ is undetectable on the background of E_B in Eq. (28), so that our numerical results for $E_B(d)$ at such σ are dominated by the regular contribution

$$E_B = C(d_c - d) + C_1(d_c - d)^2 + \cdots . \tag{49}$$

Accordingly, at $\sigma \leq 0.1$ we deduced d_c from the fit of $E_B(d)$ to a quadratic polynomial. Additionally, we confirmed that at $\sigma=0.2$ the two fitting procedures give similar results: $d_c = 0.59 \pm 0.01$ per Eq. (48) vs $d_c = 0.58 \pm 0.01$ per Eq. (49).

Finally, we have computed the electron and hole densities in the biexciton as a function of their distance from the center of mass. Examples are presented in Fig. 6 for $d=0.0$ and $d=0.3$. In the latter case the particles are on average farther away from the center of mass. The same trend is also seen in the average root-mean-square separations between various particles, which are plotted in Fig. 7. Their accelerated growth with d occurs because the biexciton becomes less bound and eventually dissociates.

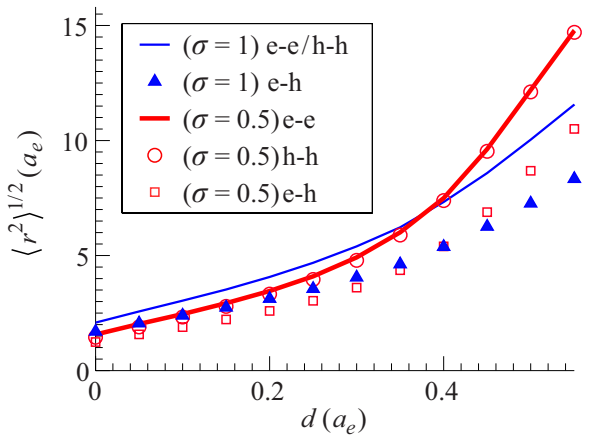

FIG. 7. (Color online) Root mean square of the pairwise distances between the biexciton constituents vs d for $\sigma=0.5$ and $\sigma=1$. Here e-e, h-h, and e-h are, respectively, electron-electron, hole-hole, and electron-hole distances.

IV. DISCUSSION

Let us compare our results with previous theoretical work. Early studies of the biexcitons based on Hartree-Fock[23] or Heitler-London[35] approximations provided initial evidence for the existence of a finite threshold d_c for the biexciton dissociation. However, they gave a considerably lower d_c than what we find here because these approximations did not account for all correlation effects essential to the biexciton stability.

Comparing with more recent calculation[17] of the biexciton binding energies by the DMC technique, we find overall excellent agreement. Still, our SVM occasionally slightly outperforms the DMC; see Table I. By this we mean that the SVM is able to find a higher E_B at some d. Indeed, since the SVM is variational and the single-exciton energy E_X is computed extremely accurately, exact E_B can only be higher than what we have found. A related property of the SVM, which speaks of its advantage over Monte Carlo methods, is the monotonic decrease in the ground-state energy at each step, so that the statistical noise is never an issue.

Neither the SVM nor the DMC is able to compute arbitrarily small binding energies; therefore, in order to determine d_c, an extrapolation to $E_B=0$ is necessary. The clarification of what extrapolation formula should be used for this purpose is an important finding of this work. Equation (48) represents the true asymptotic behavior in the limit of small E_B and indeed describes our numerical results at such E_B better than interpolation formula (10) plotted alongside for reference.

Another recent theoretical work on biexcitons used a Born-Oppenheimer-type approximation, which differs from the usual adiabatic BOA [Eq. (35)] by the replacements

$$1+\sigma \to 1, \quad U_{\mathrm{BOA}}(R) \to \frac{1}{1+\sigma} U_{\mathrm{BOA}}\left(\frac{R}{1+\sigma}\right). \tag{50}$$

Thus, both the kinetic and interaction terms are reduced by the factor of $1+\sigma$. In addition, the interaction potential is expanded in the radial direction by the same factor. The mo-

tivation for these changes was to preserve the electron-hole symmetry [Eq. (9)] and the correct single-exciton binding energy E_X at infinite separation.[36]

While the adiabatic BOA is known to give a strict lower bound[37] for the ground-state energy, no such statement can be made about the approximation of Ref. 24. As a result of this approximation, the kinetic energy is further underestimated. The potential energy is overestimated, at least, at large exciton separations, where replacement (50) magnifies the actual dipolar repulsion by the factor of $(1+\sigma)^2$. It seems that these opposite contributions largely balance each other: our binding energies E_B are generally close to those of Ref. 24; cf. our Fig. 2 and Fig. 5 of Ref. 24. Therefore, the large discrepancy between our and their d_c seen in Fig. 1 is again related to the manner in which the $E_B \to 0$ extrapolation was performed[36] in Ref. 24. At small mass ratios, where the approximation of Ref. 24 becomes accurate to the order $\mathcal{O}(\sigma)$, our results are in fact in good agreement.

Turning to the experimental implications of our theory, observations of biexcitons in single quantum well systems have been reported by many experimental groups.[9–16] In contrast, no biexciton signatures have ever been detected in electron-hole bilayers. Let us discuss how this can be understood based on our results.

The first point to keep in mind is that the biexciton dissociation threshold d_c plotted in Fig. 1 is a zero-temperature quantity. For the biexcitons to be observable at finite temperatures, E_B must exceed kT by some numerical factor. (As usual in dissociation reactions,[38] this factor is larger the smaller the exciton density is.) The coldest temperature demonstrated for the excitons in quantum wells is $T \sim 0.1$ K.[39] The maximum separation d_* between the 2D electron and hole layers at which biexcitons are still physically relevant in such structures can be roughly estimated from

$$E_B(d_*) = 10^{-3}\mathrm{Ry}_e. \tag{51}$$

Function $d_*(\sigma)$ is plotted as triangles in Fig. 1. In GaAs quantum wells we have[40] $\sigma \approx 0.5$ and $a_e = 10$ nm, and so $d_* \approx 4.5$ nm. In comparison, the smallest center-to-center separation that has been achieved in GaAs/AlGaAs and InGaAs/GaAs quantum wells without compromising the sample quality is at least twice as large.[8] Cold gases of indirect excitons have also been demonstrated in AlAs/GaAs structures,[18] in which d is smaller, $d=3.5$ nm. But the electron Bohr radius is also smaller, $a_e \approx 3$ nm, so, unfortunately, the dimensionless d is about the same.

A more serious obstacle to the creation and observation of biexcitons is disorder. A rough measure of disorder strength is given by the linewidth of the exciton optical emissions, which is currently ~ 1 meV, i.e., on the order of $0.1\mathrm{Ry}_e$ in GaAs. E_B becomes smaller than this energy scale as soon as d exceeds the thickness of a few atomic monolayers; see Fig. 2. Actually, if the disorder were due to a long-range random potential, it might still be possible to circumvent its influence on the measured optical linewidth by interferometric methods such as quantum beats.[11,13] In reality, a short-range random potential is probably quite significant.

One potentially promising system for the study of the biexciton stability diagram is a single wide quantum well subject to an external transverse electric field.[41] If the well is symmetric and the applied field is zero, we have $d=0$. A finite field can pull electrons and holes apart, leading to $d > 0$. Of course, for such a structure one should recalculate the stability diagram in Fig. 1 by taking into account the motion of particles in all three dimensions.

Although it is challenging to observe the binding of free indirect excitons, in experiments they can be loaded and held together in artificial traps.[42] We anticipate that the SVM can be a powerful tool for studying systems of a few trapped excitons theoretically, complementing recent Monte Carlo work.[43–45]

In conclusion, we have obtained the most accurate estimates to date of the binding energies of two-dimensional biexcitons. Future work may include a refined study of exciton-exciton scattering[24] and investigations of excitons in artificial traps and exciton systems of finite density. The absence of stable biexciton states implies that the ground state in the last case should be an "atomic" rather than a "molecular" superfluid.

ACKNOWLEDGMENTS

This work was supported by NSF Grant No. DMR-0706654. We are grateful to R. Needs for providing us with the numerical DMC results from Ref. 17 listed in Table I and to Ch. Schindler and R. Zimmermann for data from Ref. 24 plotted in Fig. 1. We thank L. Butov, F. Peeters, Ch. Schindler, L. Sham, and R. Zimmermann for valuable comments.

APPENDIX A: RIGOROUS BOUNDS FOR THE BIEXCITON BINDING ENERGY

In this appendix we give a few strict upper bounds on E_B, which enable us to prove the nonexistence of stable biexcitons at sufficiently large d. The basic logic of the proof was outlined in Sec. II A. Here we provide the technical details.

Our starting bound is

$$E_B \leq \max_R E_R, \tag{A1}$$

where

$$E_R = \text{inf spec } H_\infty - \text{inf spec } H_R \tag{A2}$$

is the binding energy of the two-electron Hamiltonian $H_R = T_R + U_R$ whose kinetic term is

$$T_R = -(1+\sigma)(\nabla_1^2 + \nabla_2^2), \tag{A3}$$

and the potential term U_R is given by Eq. (16). The Hamiltonian H_R is similar to that of the original problem [Eqs. (4)–(18)] except the holes are replaced by static charges separated by a given distance R and the electron mass is made equal to the reduced electron-hole mass.

To derive inequality (A1) we take advantage of the well-known theorem that the ground-state energy as a concave function in the strength of an arbitrary linear perturbation. (This theorem follows from the variational principle.) For our purposes we choose the perturbation in the form

$$\Delta T_j = \nabla_j^2 - \nabla_{\mathbf{R}_j}^2. \tag{A4}$$

We add it to the kinetic-energy terms with the coefficient $-\sigma \le \tau \le 1$, yielding $T_j \to T_j + \tau \Delta T_j$. Hamiltonians H and H_R are obtained by setting $\tau=0$ and $\tau=-\sigma$, respectively.

The perturbation leaves the reduced electron-hole mass invariant. Therefore, it does not affect the ground-state energy E_X of a single exciton. The energy $E_{XX}(\tau)$ does vary with τ and the aforementioned concavity property dictates that

$$E_{XX}(\tau) \ge \frac{1-\tau}{1+\sigma} E_{XX}(-\sigma) + \frac{\tau+\sigma}{1+\sigma} E_{XX}(1). \tag{A5}$$

Since $E_{XX}(-\sigma)=E_{XX}(1)$ by electron-hole symmetry, the right-hand side is equal to $E_{XX}(-\sigma)$ for all τ. Consequently, $\tau=-\sigma$ gives the largest binding energy and we arrive at inequality (A1).

If the kinetic energy T_R is discarded, E_R becomes equal to $-V_{\mathrm{cl}}(R,d)<0$. We want to ascertain that quantum corrections do not change the sign of E_R.

The quantum corrections appear in both E_X and E_{XX}. The former are well understood.[22] The internal dynamics of the exciton in the large-d case is analogous to that of a 2D harmonic oscillator with the amplitude of the zero-point motion given by

$$\langle |\mathbf{r}_1 - \mathbf{R}_1|^2 \rangle = l^2, \quad l = d^{3/4}(1+\sigma)^{1/4} \ll d. \tag{A6}$$

The corresponding energy correction is

$$E_X + \frac{2}{d} = \frac{2\sqrt{1+\sigma}}{d^{3/2}} - \mathcal{O}\left(\frac{1}{d^2}\right). \tag{A7}$$

This result immediately restricts the range of R where the stable biexciton may in principle exist. By positivity of the kinetic energy, $E_R < 2E_X - U_{\min}(R,d)$, where $U_{\min}$ is defined in Sec. II A. Therefore, $E_R>0$ may occur only at R that satisfy

$$V_{\mathrm{cl}}(R) > 2E_X + \frac{4}{d}. \tag{A8}$$

In view of Eqs. (17) and (A7), R must necessarily be much larger than d.

Choose an arbitrary d_1 such that $d \ll d_1 \ll R$. By definition of $U_{\min}$,

$$U_R \ge U_{\min}(R,d_1) + V_Y(\mathbf{r}_1) + V_Y(\mathbf{r}_2), \tag{A9}$$

$$V_Y(\mathbf{r}) = \sum_{\mathbf{t}=\pm\mathbf{R}/2} [v(\mathbf{r}-\mathbf{t},d_1) - v(\mathbf{r}-\mathbf{t},d)]. \tag{A10}$$

Accordingly, $E_R < 2E_X - U_{\min}(R,d_1) - 2E_Y$, where E_Y is the ground-state energy of a *single* electron subject to the potential $V_Y(\mathbf{r})$ of four out-of-plane charges. This potential has the shape of two symmetric wells separated by the distance R. The amplitude of the zero-point motion in each well is again $l \ll R$. Therefore, the energy shift due to tunneling between the wells is exponentially small. (A rigorous upper bound can be given.[46]) Furthermore, potential V_Y near the bottom of each well coincides with that of a single exciton up to a constant

$$\Delta V_Y = V_Y\left(\frac{\mathbf{R}}{2}\right) - \frac{2}{d} = \frac{2}{d_1} + \frac{d_1^2 - d^2}{R^3}. \tag{A11}$$

Hence, $E_Y = E_X + \Delta V_Y$ and

$$E_R \le -\frac{2d^2}{R^3} - \left[V_{\mathrm{cl}}(R,d_1) - \frac{2d_1^2}{R^3} \right]. \tag{A12}$$

In these formulas we have dropped subleading terms $o(l^2/d_1^2)$, $o(d_1^4/R^5)$, etc. With the same accuracy the bracket in Eq. (A12) vanishes [cf. Eq. (17)], so that we arrive at the result $E_R \simeq -V_{\mathrm{cl}}(R,d)$. This simply means that at large d all quantum corrections to E_R are parametrically smaller than the direct dipolar repulsion of the two excitons. Therefore, $E_R \le 0$ at all R, so that $E_B \le 0$, and the proof is complete.

APPENDIX B: RADIAL WAVE FUNCTION FOR SMALL MASS RATIOS

In this appendix we show how the suitable solution of Eq. (36) can be constructed within the quasiclassical approximation. The necessary connection formulas are derived by asymptotic matching with two exact solutions at small and large R.

It is convenient to define the rescaled wave function $\psi(R) = \chi(R)\sqrt{R}$. From Eq. (36) we find that ψ satisfies the equation

$$\psi'' - \left(\varkappa^2 + \mu V(R) - \frac{1}{4R^2} \right) \psi = 0. \tag{B1}$$

This equation has two linearly independent quasiclassical solutions,

$$\psi_\pm(R) = \frac{1}{\sqrt{Q(R)}} \exp\{\pm[S(R) - S(b)]\}, \tag{B2}$$

where Q and S are given by

$$Q(R) = \sqrt{\varkappa^2 + \mu V(R)}, \quad S(R) = \int_{R_+}^{R} d\rho Q(\rho). \tag{B3}$$

The subtraction of the R-independent term $S(b)$ in the exponentials amounts to multiplying $\psi_\pm$ by unimportant constants. This is done for the sake of convenience. The centrifugal barrier $1/4R^2$ in the formula for Q is dropped because we need the quasiclassical solution only at $\sigma \ll R \ll b$ where $\mu[V(R) - V(R_0)] \gg 1/4R^2$. Here $R_0 = (R_+ + R_-)/2$ is the point where the potential $V(R)$ has the minimum. (Actually, if we wished to use the quasiclassical method at $R \ll \sigma$, dropping the centrifugal barrier would indeed be necessary in order to compensate for the well-known inaccuracy of this approximation near the origin.[47])

In the following we assume that $\varkappa \ll 1/b$, in which case there exists a broad interval $d \ll R \ll b$ where potential $V(R)$ is dominated by dipolar repulsion (1). In this interval, $\mu V(R) \simeq b/4R^3 \gg \varkappa^2$; therefore,

$$\psi_\pm(R) \simeq \left(\frac{4}{b}R^3\right)^{1/4} \exp\left[\pm \left(1 - \sqrt{\frac{b}{R}} \right) \right]. \tag{B4}$$

Using the asymptotic expansion formulas[28] for I_0 and K_0, it is easy to see that the linear combination

$$\psi(R) \simeq \frac{e}{2\sqrt{\pi}}\psi_-(R) - \frac{2\sqrt{\pi}}{e}c_2\psi_+(R) \tag{B5}$$

of the quasiclassical wave functions in Eq. (B4) smoothly matches with exact solution (38) at $d \ll R \ll b$. This is our first connection formula. It is crucial for this derivation because in the intermediate range of distances $b \ll R \ll \varkappa$ the quasiclassical approximation breaks down. (It is invalidated by the sharp decrease in V with R.) In that region $\chi(R)=\psi/\sqrt{R}$ exhibits a slow logarithmic falloff [Eq. (25)] instead of the algebraic decay suggested by Eq. (B4). As explained in Sec. II, nonanalytical behavior (12) of the binding energy is precisely due to this logarithmic falloff.

To finish the calculation we need a second connection formula between χ given by Eq. (B5) and the same function near the classical turning point R_+. To find it we take advantage of the exact solution for harmonic-oscillator potential (39) in terms of the parabolic cylinder function,[28]

$$\psi \propto D_{\varepsilon-1/2}(-\sqrt{2}x), \quad x = \frac{R-R_0}{l}, \tag{B6}$$

where $l=(2/\mu V'')^{1/4}$ is the amplitude of zero-point motion about this minimum, and ε, given by

$$\varepsilon = \frac{1}{2}l^2[\mu|V(R_0)| - \varkappa^2], \tag{B7}$$

is the corresponding energy in units of the oscillator frequency $\omega=2/\mu l^2$. For the ground state we expect

$$\delta \equiv \varepsilon - \frac{1}{2} \ll 1. \tag{B8}$$

The negative sign in the argument of $D_{\varepsilon-1/2}$ in Eq. (B6) is chosen to obtain an exponentially decaying wave at large negative x, i.e., from the left turning point R_- and toward the origin. At large positive x, that is, at $R-R_+ \gg l$, both decaying and growing exponentials are present. At such x the wave function can be cast into the quasiclassical form

$$\psi \simeq \sum_{\nu=\pm}\frac{c_\nu}{\sqrt{x}}\exp\left(\nu\int_{\sqrt{2\varepsilon}}^{x} d\xi\sqrt{\xi^2-2\varepsilon}\right), \tag{B9}$$

which is equivalent to

$$\sqrt{l}\psi(R) \simeq c_-e^{-S(b)}\psi_-(R) + c_+e^{S(b)}\psi_+(R). \tag{B10}$$

See Eqs. (39), (B2), and (B6). This is our second connection formula except that we still have to specify the preexponential factors c_+ and c_-. In fact, only their ratio is important. With the help of the asymptotical expansion[28] for D_δ, one finds it to be[48]

$$\frac{c_+}{c_-} \simeq -2\sqrt{\pi e}\,\delta. \tag{B11}$$

Comparing Eqs. (B5) and (B10), we obtain

$$\delta \simeq -\frac{1}{2\sqrt{\pi e}}\frac{c_+}{c_-} \simeq 2\sqrt{\frac{\pi}{e}}c_2e^{-2S(b)-2}. \tag{B12}$$

For $\varkappa$ at which the above calculation is valid, we have $S(b) \simeq S_0-1$, where $S_0=S(R=\infty,\varkappa=0)$. Thus, we arrive at

$$\varkappa^2 \simeq \mu|V(R_0)| - \frac{1}{l^2} - 4\sqrt{\frac{\pi}{e}}\frac{c_2}{l^2}e^{-2S_0}, \tag{B13}$$

which leads to Eqs. (40)–(42) of Sec. II.

Finally, a minor technical comment is in order. Since we have used the quasiclassical approximation, all coefficients in Eq. (B13) have a relative accuracy $\mathcal{O}(e^{-S(b)})$. In particular, we expect that in place of $V(R_0)$ we have a slightly more negative value, so that the ground-state energy $-E_B$ never exceeds the oscillator ground-state energy $V(R_0)+1/(2\mu l^2)$, as required by physical considerations.

[1] M. Hagn, A. Zrenner, G. Böhm, and G. Weimann, Appl. Phys. Lett. **67**, 232 (1995).
[2] A. V. Larionov, V. B. Timofeev, J. Hvam, and K. Soerensen, Zh. Eksp. Teor. Fiz. **117**, 1255 (2000) [JETP **90**, 1093 (2000)].
[3] L. V. Butov, A. C. Gossard, and D. S. Chemla, Nature (London) **418**, 751 (2002).
[4] Z. Vörös, R. Balili, D. W. Snoke, L. Pfeiffer, and K. West, Phys. Rev. Lett. **94**, 226401 (2005).
[5] A. L. Ivanov, L. E. Smallwood, A. T. Hammack, Sen Yang, L. V. Butov, and A. C. Gossard, Europhys. Lett. **73**, 920 (2006).
[6] A. A. High, E. E. Novitskaya, L. V. Butov, M. Hanson, and A. C. Gossard, Science **321**, 229 (2008).
[7] S. Yang, A. T. Hammack, M. M. Fogler, L. V. Butov, and A. C. Gossard, Phys. Rev. Lett. **97**, 187402 (2006); M. M. Fogler, Sen Yang, A. T. Hammack, L. V. Butov, and A. C. Gossard, Phys. Rev. B **78**, 035411 (2008).
[8] L. V. Butov, J. Phys.: Condens. Matter **19**, 295202 (2007).
[9] R. C. Miller, D. A. Kleinman, A. C. Gossard, and O. Munteanu, Phys. Rev. B **25**, 6545 (1982).
[10] R. T. Phillips, D. J. Lovering, G. J. Denton, and G. W. Smith, Phys. Rev. B **45**, 4308 (1992).
[11] S. Bar-Ad and I. Bar-Joseph, Phys. Rev. Lett. **68**, 349 (1992).
[12] D. Birkedal, J. Singh, V. G. Lyssenko, J. Erland, and J. M. Hvam, Phys. Rev. Lett. **76**, 672 (1996).
[13] S. Adachi, T. Miyashita, S. Takeyama, Y. Takagi, A. Tackeuchi, and M. Nakayama, Phys. Rev. B **55**, 1654 (1997).
[14] J. C. Kim and J. P. Wolfe, Phys. Rev. B **57**, 9861 (1998).
[15] W. Langbein and J. M. Hvam, Phys. Status Solidi A **190**, 167 (2002).
[16] M. Maute, S. Wachter, H. Kalt, K. Ohkawa, and D. Hommel, Phys. Rev. B **67**, 165323 (2003).
[17] M. Y. J. Tan, N. D. Drummond, and R. J. Needs, Phys. Rev. B **71**, 033303 (2005).
[18] L. V. Butov and A. I. Filin, Phys. Rev. B **58**, 1980 (1998).
[19] D. Bressanini, M. Mella, and G. Morosi, Phys. Rev. A **57**, 4956 (1998).
[20] J. Usukura, Y. Suzuki, and K. Varga, Phys. Rev. B **59**, 5652 (1999).

[21] C. Riva, F. M. Peeters, K. Varga, and V. A. Schweigert, Phys. Status Solidi B **234**, 50 (2002), and references therein.
[22] Y. E. Lozovik and O. L. Berman, Zh. Eksp. Teor. Fiz. **111**, 1879 (1997) [JETP **84**, 1027 (1997)].
[23] S. Ben-Tabou de-Leon and B. Laikhtman, Europhys. Lett. **59**, 728 (2002).
[24] Ch. Schindler and R. Zimmermann, Phys. Rev. B **78**, 045313 (2008); R. Zimmermann and Ch. Schindler, Solid State Commun. **144**, 395 (2007).
[25] L. D. Landau and E. M. Lifshitz, *Quantum Mechanics: Nonrelativistic Theory* (Pergamon, New York, 1965).
[26] K. Varga and Y. Suzuki, Phys. Rev. C **52**, 2885 (1995).
[27] Y. Suzuki and K. Varga, *Stochastic Variational Approach to Quantum-Mechanical Few-Body Problems*, Lecture Notes in Physics Vol. M54 (Springer, Berlin, 1998), pp. 1–310.
[28] I. S. Gradshteyn and I. M. Ryzhik, in *Table of Integrals, Series, and Products*, 6th ed., edited by A. Jeffrey and D. Zwillinger (Academic, San Diego, 2000).
[29] D. Bollé and F. Gesztesy, Phys. Rev. Lett. **52**, 1469 (1984); Phys. Rev. A **30**, 1279 (1984).
[30] M. Born and J. R. Oppenheimer, Ann. Phys. **84**, 457 (1927).
[31] M. Born, *Festschrift Göttinger Akademie der Wissenschaften, I: Math.-Phys. Klasse 1* (1951); M. Born and H. Huang, *Dynamical Theory of Crystal Lattices* (Oxford University Press, New York, 1998).
[32] To this end one can iteratively diagonalize the four-body biexciton Hamiltonian H_{XX} by a sequence of canonical transformations (Refs. 49 and 50). Equivalently, in the Lagrangian formalism, one would integrate out two out of four fermion degrees of freedom. This generates corrections to the potential and kinetic terms of Eq. (36).
[33] J. Adamowski, S. Bednarek, and M. Suffczynski, Solid State Commun. **9**, 2037 (1971).
[34] K. Varga and Y. Suzuki, Comput. Phys. Commun. **106**, 157 (1997); the companion computer program is available at the CPC Program Library, online at http://www.cpc.cs.qub.ac.uk
[35] S. Okumura and T. Ogawa, Phys. Rev. B **65**, 035105 (2001).
[36] Ch. Schindler and R. Zimmermann, private communication.
[37] R. T. Pack and J. O. Hirschfelder, J. Chem. Phys. **52**, 521 (1970).
[38] M. N. Saha, Proc. R. Soc. London, Ser. A, **99**, 135 (1921).
[39] L. V. Butov, A. L. Ivanov, A. Imamoglu, P. B. Littlewood, A. A. Shashkin, V. T. Dolgopolov, K. L. Campman, and A. C. Gossard, Phys. Rev. Lett. **86**, 5608 (2001).
[40] L. V. Butov, A. V. Mintsev, Yu. E. Lozovik, K. L. Campman, and A. C. Gossard, Phys. Rev. B **62**, 1548 (2000).
[41] L. Schultheis, K. Köhler, and C. W. Tu, Phys. Rev. B **36**, 6609 (1987).
[42] A. T. Hammack, N. A. Gippius, Sen Yang, G. O. Andreev, L. V. Butov, M. Hanson, and A. C. Gossard, J. Appl. Phys. **99**, 066104 (2006).
[43] E. Anisimovas and F. M. Peeters, Phys. Rev. B **71**, 115319 (2005).
[44] E. Anisimovas and F. M. Peeters, Phys. Rev. B **74**, 245326 (2006).
[45] A. Filinov, M. Bonitz, P. Ludwig, and Yu. E. Lozovik, Phys. Status Solidi C **3**, 2457 (2006).
[46] Ph. Briet, J. M. Combes, and P. Duclos, Commun. Math. Phys. **126**, 133 (1989).
[47] M. V. Berry and A. M. Ozorio de Almeida, J. Phys. A **6**, 1451 (1973).
[48] S. C. Miller and R. H. Good, Phys. Rev. **91**, 174 (1953).
[49] P. R. Bunker and R. E. Moss, Mol. Phys. **33**, 417 (1977).
[50] S. Weigert and R. G. Littlejohn, Phys. Rev. A **47**, 3506 (1993).